
Article:
Cummings, James and Karadakov, Peter Borislavov orcid.org/0000-0002-2673-6804 (2023) Aromaticity in the Electronic Ground and Lowest Triplet States of Molecules with Fused Thiophene Rings. Chemistry : A European Journal. e202303724. ISSN: 0947-6539

https://doi.org/10.1002/chem.202303724

Chemistry–A European Journal
Research Article
doi.org/10.1002/chem.202303724
Chemistry Europe
European Chemical Societies Publishing
www.chemeurj.org

Aromaticity in the Electronic Ground and Lowest Triplet States of Molecules with Fused Thiophene Rings

Edward Cummings[a] and Peter B. Karadakov*[a]

Analysis of the variations of the off-nucleus isotropic magnetic shielding, $\sigma_{iso}(\mathbf{r})$, around thiophene, thienothiophenes, dithienothiophenes and sulflowers in their electronic ground (S_0) and lowest triplet (T_1) states reveals that some of the features of aromaticity and bonding in these molecules do not fit in with predictions based on the popular Hückel's and Baird's rules. Despite having $4n$ π electrons, the S_0 states of the sulflowers are shown to be aromatic, due to the local aromaticities of the individual thiophene rings. To reduce its T_1 antiaromaticity, the geometry of thiophene changes considerably between S_0 and T_1: In addition to losing planarity, the carbon-carbon two 'double' and one 'single' bonds in S_0 turn into two 'single' and one 'double' bonds in T_1. Well-defined Baird-style aromaticity reversals are observed between the S_0 and T_1 states of only three of the twelve thiophene-based compounds investigated in this work, in contrast, the sulflower with six thiophene rings which is weakly aromatic in S_0 becomes more aromatic in T_1. The results suggest that the change in aromaticity between the S_0 and T_1 states in longer chains of fused rings is likely to affect mostly the central ring (or the pair of central rings); rings sufficiently far away from the central ring(s) can retain aromatic character.

Introduction

Enhancing the understanding of aromaticity is of benefit to many areas of chemical research because of the ubiquity of aromatic compounds. Aromatic compounds are all around us, for example, DNA and RNA sequences are comprised of five nucleotides, all of which are aromatic; enormous quantities of aromatic compounds are produced and processed annually – these can be found in manufactured polymers, for example, polyesters,[1] and in fuels, for example, petrol[2] and diesel.[3] Interest in thiophene-containing heteroaromatic compounds such as polythiophenes is associated with their wide range of potential applications which include organic field effect transistors (OFETs)[4–7] and organic light-emitting diodes (OLEDs).[8] In this paper we examine aromaticity and bonding in compounds with fused thiophene rings some of which have attracted the attention of astrochemists. Over the past decade, thiophene-containing compounds have been found by NASA's Mars Curiosity Rover,[9–11] during the quest to find Martian biosignatures.[10] In general, aromatic molecules are stable, in contrast to antiaromatic molecules which have much smaller HOMO–LUMO gaps[12–14] and singlet-triplet separations[15] and, as a consequence, are less stable. The π electrons in compounds with condensed thiophene rings can traverse alternative conjugation pathways which makes establishing the levels of aromaticity in the singlet ground (S_0) and lowest triplet (T_1) electronic states of these compounds a non-trivial task.

Even the aromaticity of thiophene **1** (Figure 1) is a challenge to quantify, as it is known to be more aromatic than pyrrole (where sulfur is substituted for nitrogen) and furan (where the heteroatom is oxygen).[16] In each of these five-membered heteroaromatics, the heteroatom donates two electrons to the π system, circumventing the need to have a sixth atom in the conjugated ring in order to have a $4n+2$ Hückel aromatic π system similar to that in benzene. Four isomers can be formed by condensing two thiophene rings, namely, thieno[2,3-*b*]thiophene **2**, thieno[3,2-*b*]thiophene **3**, thieno[3,4-*b*]thiophene **4** and thieno[3,4-*c*]thiophene **5**; all of these are examined in this paper. Thieno[2,3-*b*]thiophene **2** has a central cross-conjugated 'double' bond which prevents the establishment of a conjugation pathway involving three carbon-carbon π bonds. Consequently, its HOMO-LUMO gap is higher than those of thieno[3,2-*b*]thiophene **3** and thieno[3,4-*b*]thiophene **4**, where the longer conjugation pathways lead to lower HOMO-LUMO gaps.[17] Due to the variation in the lengths of the conjugation pathways, relative stability and electron-rich nature, the first three thienothiophenes provide useful building blocks for constructing organic semiconductors.[18] The fourth thienothiophene, thieno[3,4-*c*]thiophene **5**, which has resonance structures involving a sulfur atom with a formal oxidation state of +4, is far less stable and has not been isolated in unsubstituted form.

There are twelve dithienothiophene isomers; each of these involves three condensed thiophene rings. In this paper we examine two of these isomers, dithieno[3,2-*b*;2′,3′-*d*]thiophene **6** and dithieno[2,3-*b*:3′,2′-*d*]thiophene **7**. Dithienothiophenes appear as intermediates in a number of reactions[19] and can be used as materials for p-type semiconductors in OFETs, due to their planar, sulfur-rich, rigid, conjugated and highly thermally

[a] E. Cummings, Prof. Dr. P. B. Karadakov
Department of Chemistry, University of York
Heslington, York YO10 5DD, UK
E-mail: peter.karadakov@york.ac.uk

Supporting information for this article is available on the WWW under https://doi.org/10.1002/chem.202303724

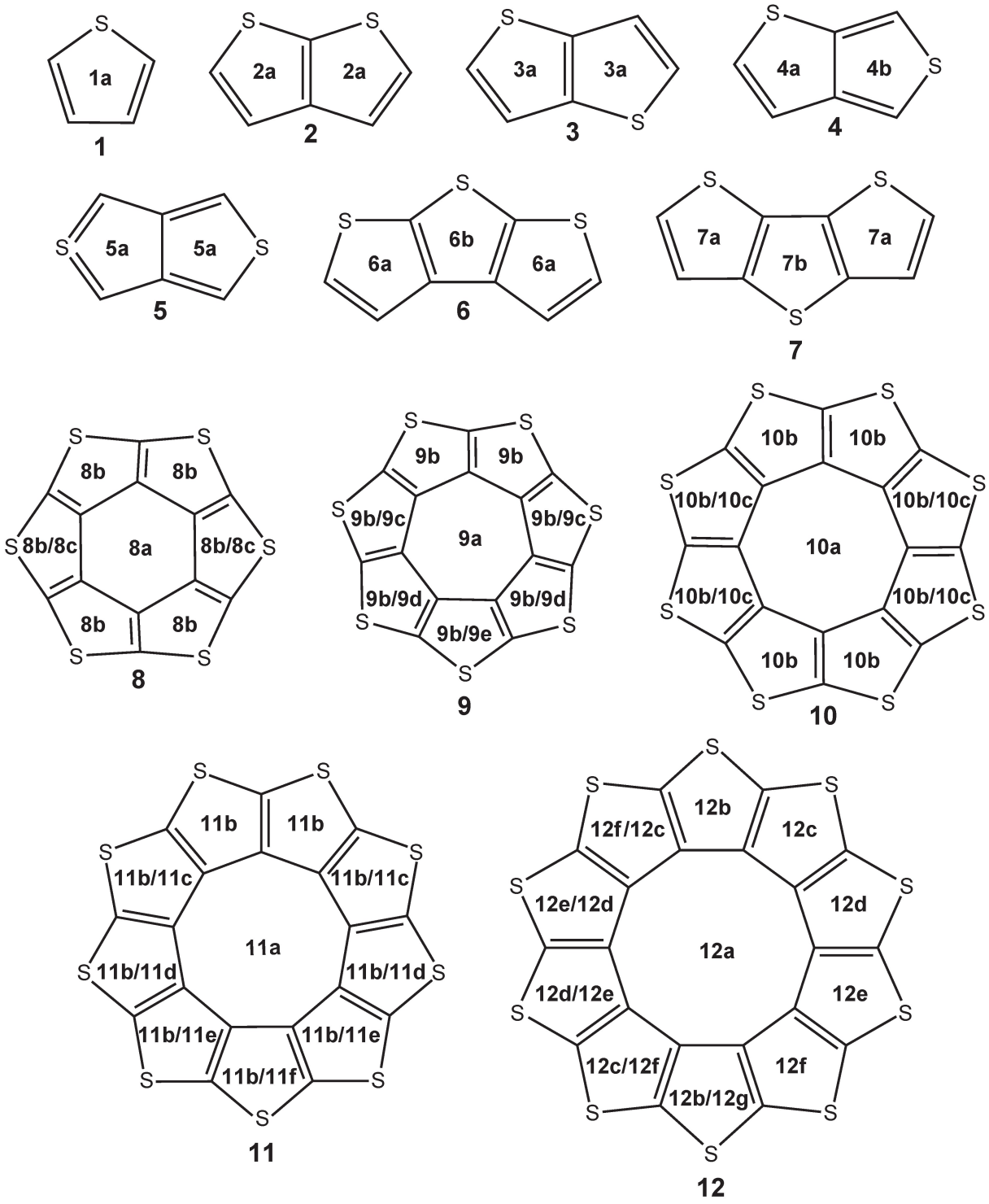

Figure 1. Thiophene **1**, thieno[2,3-*b*]thiophene **2**, thieno[3,2-*b*]thiophene **3**, thieno[3,4-*b*]thiophene **4**, thieno[3,4-*c*]thiophene **5**, dithieno[2,3-*b*:3′,2′-*d*]thiophene **6** and dithieno[3,2-*b*;2′,3′-*d*]thiophene **7**; sulflowers with six **8**, seven **9**, eight **10**, nine **11** and ten **12** C_2S units, $(C_2S)_6$—$(C_2S)_{10}$. All rings are labelled by structure numbers followed by letters; rings related through symmetry operations share the same label. Ring labels that differ between the S_0 and T_1 optimised geometries are separated by a slash '/', with the S_0 label first.

stable and photostable structures.[17] Some dithienothiophenes are available commercially.[20]

Recent studies of systems involving interconnected heterocycles have shown that these can feature alternative cyclic conjugation pathways with $4n+2$ or $4n$ π electrons, exhibiting competing aromatic and antiaromatic properties.[21,22] Condensed thiophene rings can form a class of heterocirculenes known as 'sulflowers',[23] with a molecular formula $(C_2S)_n$. A

sulflower can be viewed as constructed from an 'outer' $(CS)_n$ ring formed by carbon-sulfur rim bonds and an 'inner' C_n ring formed by carbon-carbon hub bonds; these rings are connected by carbon-carbon 'double' spoke bonds which create opportunities for the establishment of a number of cyclic conjugation pathways. In this paper we investigate sulflowers with 6, 7, 8, 9 and 10 condensed thiophene rings: hexathio[6]circulene **8**, heptathio[7]circulene **9**, octathio[8]circulene **10**, nonathio[9]circulene **11** and decathio[10]circulene **12**. The most stable of these sulflowers is thought to be $(C_2S)_8$ **10** which has been shown to have the lowest energy per repeat unit.[23,24] Computational studies of more strained sulflowers with 4, 5, 11 and 12 condensed thiophene rings have been carried out by other authors.[24,25] Dianions and dications of $(C_2S)_8$ and other hetero[8]circulenes are thought to have increased stability due to the establishment of a $4n+2$ Hückel-aromatic π system involving the 'inner' C_8 ring.[26] Further research on sulflowers and similar circulenes[27] has investigated replacing sulfur with other substituents such as oxygen,[28] selenium and tellurium,[24] as well as broader aspects of the structure and reactivity of heterocirculenes[26,29] and their synthesis.[30–32]

Aromaticity in the electronic ground and excited states of cyclic conjugated systems is usually associated with two π electron counting rules: Hückel's familiar classification of systems with $4n+2$ and $4n$ π electron systems as aromatic and antiaromatic, respectively,[33–35] and Baird's rule, according to which Hückel's classification is reversed in the lowest vertical $\pi\pi^*$ triplet state so that systems with $4n$ π electrons become aromatic while those with $4n+2$ π electrons become antiaromatic.[36]

Structurally, the sulflowers $(C_2S)_6$–$(C_2S)_{10}$ (**8**–**12** in Figure 1) resemble two well-known polycyclic aromatic hydrocarbons (PAHs), coronene ($C_{24}H_{12}$) and corannulene ($C_{20}H_{10}$), which have 24 and 20 π electrons, respectively, and so, while aromatic, do not formally conform to Hückel's $4n+2$ rule. Similarly, each C_2S unit in a sulflower with a molecular formula $(C_2S)_n$ contributes four π electrons, hence the total number of π electrons is $4n$. This suggests that it would be more appropriate to look at the aromaticities of the individual thiophene rings, and of the $(CS)_n$ rim and C_n hub rings, rather than at the total π electron counts. All individual thiophene rings in **8**–**12** should be aromatic; the rim and hub rings could be thought of as the components of an 'annulene-within-a-heteroannulene' model analogous to the 'annulene-within-an-annulene' (AWA) model[37,38] suggested in order to explain the aromaticity of corannulene but strongly questioned by subsequent research.[39] According to Baird's rule, some of the individual thiophene rings, as well as the rim and hub rings and could be expected to experience aromaticity reversals in the T_1 state. Clearly, establishing the levels of aromaticity in the electronic ground and excited states of polycyclic conjugated compounds could require more detailed analysis going way beyond straightforward applications of Hückel's and Baird's rules to various cyclic conjugation pathways with $4n+2$ or $4n$ π electrons. There are well-known examples of molecules with condensed rings exhibiting local aromaticity and local antiaromaticity, respectively, in their electronic ground states such as benzocyclobutadiene[40–44] and biphenylene.[42,43,45,46] Recent studies have suggested the existence of Hückel aromatic character in the T_1 states of Cibalackrot-type compounds[47] and mixed Hückel-Baird hybrid aromatic character in the T_1 states of pro-aromatic quinoidal compounds.[48]

Quantifying and, in some cases, even identifying aromaticity, can be far from straightforward – this has led to the formulation of a number of structural, energetic, reactivity-based, electron delocalisation and magnetic aromaticity criteria. Many of these criteria, for example, bond resonance energy (BRE),[49–55] topological resonance energy (TRE),[56–58] circuit resonance theory (CRE),[59–62] gauge-including magnetically induced currents (GIMIC),[63] are theoretical and are not linked directly to experimentally verifiable observables. Structural aromaticity criteria, for example, the harmonic oscillator measure of aromaticity (HOMA)[64,65] and the Bird index[66] work by comparing bond lengths to predetermined values for aromatic systems and are straightforward to calculate. While HOMA is known to perform well for the electronic ground states of benzenoid compounds[67] and a strong correlation has been observed between HOMA values and magnetic criteria for the electronic ground states of compounds of this type,[68] HOMA needs to be re-parametrised[69] in order to produce more reliable aromaticity predictions for molecules in another electronic state such as T_1. We report values of the HOMA and Bird indices for the S_0 and T_1 states of the sulflowers studied in this paper, using electronic ground state parameters throughout, and we argue that these indices do not work sufficiently well for this type of compound (see the Supporting Information).

The main tools that we use to analyse aromaticity and bonding in the S_0 and T_1 states of the compounds with condensed thiophene rings studied in this paper are based on the calculation of magnetic shielding tensors, $\boldsymbol{\sigma}(\mathbf{r})$, evaluated at various positions $\mathbf{r}$ within the space surrounding a molecule, and not just at nuclear positions as required when interpreting NMR experimental data. Off-nucleus isotropic magnetic shieldings, $\sigma_{iso}(\mathbf{r}) = \frac{1}{3}[\sigma_{xx}(\mathbf{r}) + \sigma_{yy}(\mathbf{r}) + \sigma_{zz}(\mathbf{r})]$, and out-of-plane components of $\boldsymbol{\sigma}(\mathbf{r})$, $\sigma_{zz}(\mathbf{r})$, are involved in the definitions of nucleus-independent chemical shifts (NICS), popular single-point aromaticity indices introduced by Schleyer and coworkers.[42,70] The original NICS index for a planar ring, NICS(0), was defined as $-\sigma_{iso}$(at ring center); subsequent attempts to improve the accuracy of relative aromaticity predictions led to the formulation of further NICS indices including NICS(1) $= -\sigma_{iso}$(at 1 Å above ring center), NICS$(0)_{zz} = -\sigma_{zz}$(at ring center) and NICS$(1)_{zz} = -o_{zz}$ (at 1 Å above ring center).

Some of the sulflower geometries studied in this paper are planar, but the majority are bowl-shaped. Calculating NICS(0) for the rings making up nonplanar sulflowers is not a problem because the centre of a non-planar ring can be located by averaging the coordinates of its atoms; in order to calculate NICS values above and below that ring, a plane is fitted to the coordinates of the ring atoms and ring centre and NICS($\pm$1) values are calculated at the points 1 Å above and below that plane along the normal passing through the ring centre following the procedure outlined in refs. [71] and [72]. For a

non-planar ring, these two points are usually not equivalent by symmetry and the NICS(±1) values are different; we select NICS(−1) as the smaller of the two values, for bowl-shaped molecules NICS(−1) and NICS(+1) correspond to positions inside and outside the bowl, respectively.

Certain aspects of the NICS approach have been subject to criticism; one of these is associated with the fact that, for now, NICS (just as any off-nucleus shielding and ring currents) cannot be measured experimentally.[73] Moreover, for single-point quantities such as NICS the locations at which these quantities are calculated are chosen in a more or less arbitrary manner; NICS can exhibit strong positional dependence and, in certain situations, standard choices can be inappropriate.[74,75] Research on ring currents[76,77] suggests that the reduction of a global molecular property such as the current density map to a single NICS value could lead to significant loss of information; this makes it difficult to distinguish between systems which have similar NICS values but exhibit quite different ring currents. In this context, it is clearly more appropriate to study not just NICS calculated at selected points in space, but the overall behaviour of the off-nucleus isotropic shielding, at a similar level of detail as current density maps. The approach we use to investigate aromaticity and bonding in sulflowers is close in spirit to the work of Wolinski[78] who analyzed the changes in the off-nucleus shielding tensor along the molecular axes of linear molecules and to the isotropic shielding isosurfaces investigated by Klod and Kleinpeter.[79] It has been shown (see ref. [80] and references therein) that accurate $\sigma_{iso}(\mathbf{r})$ isosurfaces and contour plots constructed using fine grids of points can be used not only to distinguish between aromatic and antiaromatic systems, such as benzene and cyclobutadiene, but also to characterise chemical bonds and investigate the extents to which these bonds are affected by the aromatic or antiaromatic nature of the molecule in which they reside. The application of this approach to the S_0 and T_1 states of the compounds with condensed thiophene rings studied in this paper reveals, in detail, the differences in aromaticity and the specific features of bonding in these molecules in the two electronic states.

Computational Details

The S_0 geometries of molecules **1–12** were optimised at the RB3LYP-D3(BJ)/def2-TZVP level (restricted B3LYP[81–84] with Grimme's D3 empirical dispersion corrections and Becke-Johnson damping,[85] within the def2-TZVP[86] basis set); the respective T_1 geometries were optimised at the unrestricted UB3LYP-D3(BJ)/def2-TZVP level. All optimised geometries were confirmed as local minima through analytical harmonic frequency calculations.

The C_{2v} symmetry of the optimised electronic ground state geometry of thiophene **1** is reduced to C_s in the respective geometry of its lowest triplet state; this is accompanied by an out-of-plane bending of the hydrogen atoms in the same direction. The thienothiophene in which the sulfur atoms are arranged as in the sulflowers, thieno[2,3-*b*]thiophene **2**, has an S_0 optimised geometry of C_{2v} symmetry, and a T_1 optimised geometry of C_2 symmetry; the symmetry reduction involves an out-of-plane bending of the hydrogen atoms which, in contrast to that observed in thiophene, is in opposite directions for the pairs of hydrogen atoms from the two thiophene rings. The optimised geometries of both the S_0 and T_1 states of thieno[3,2-*b*]thiophene **3** and thieno[3,4-*b*]thiophene **4** were found to be of C_s symmetry. There is no change in the D_{2h} symmetry of the optimised geometries of thieno[3,4-*c*]thiophene **5** between S_0 and T_1. The optimised geometry of the next sulflower precursor, dithieno[2,3-*b*:3′,2′-*d*]thiophene **6**, switches from C_{2v} symmetry in S_0 to C_2 symmetry in T_1, with a loss of planarity. The symmetry reductions on passing from S_0 to T_1 in **2** and **6** suggest that the T_1 states of sulflowers can be expected to show similar distortions of the respective T_1 optimised geometries. The S_0 and T_1 optimised geometries of dithieno[3,2-*b*;2′,3′-*d*]thiophene **7** were found to be of the same C_{2v} symmetry.

Looking at the sulflowers, the S_0 optimised geometries of $(C_2S)_6$ **8** and $(C_2S)_7$ **9** were found to be bowl-shaped, of C_{6v} and C_{7v} symmetry, respectively; those of $(C_2S)_8$ **10** and $(C_2S)_9$ **11** were found to be planar, of D_{8h} and D_{9h} symmetry, respectively; that of $(C_2S)_{10}$ **12** was found to be of corrugated shape and of C_2 symmetry. The symmetries of the T_1 optimised geometries of the sulflowers studied in this paper turned out to be significantly lower than those of their S_0 counterparts, namely C_{2v} for $(C_2S)_6$ and $(C_2S)_8$, and C_s for $(C_2S)_7$, $(C_2S)_9$ and $(C_2S)_{10}$, which is an indication of attempts to decrease energy by lowering symmetry. As a consequence, the T_1 optimised geometries of $(C_2S)_6$, $(C_2S)_7$, $(C_2S)_8$, $(C_2S)_9$ and $(C_2S)_{10}$ include 3, 4, 2, 5 and 6 symmetry-unique thiophene rings, respectively, in contrast to the S_0 optimised geometries, amongst which only that of $(C_2S)_{10}$ features more than one symmetry-unique thiophene ring (the number of such rings in the electronic ground state of this sulflower is five).

Our S_0 optimised lengths of the carbon-sulfur rim, carbon-carbon hub and carbon-carbon 'double' spoke S_0 bonds in $(C_2S)_8$ **10**, 1.752, 1.417 and 1.381 Å, respectively, provide an almost perfect match for the experimentally measured bond lengths of 1.751, 1.419 and 1.380 Å.[23,24,87]

NICS values and volume data required to construct S_0 isotropic shielding isosurfaces were obtained through RB3LYP-GIAO/6-311++G(d,p) calculations [RB3LYP with gauge-including atomic orbitals,[88–92] within the 6-311++G(d,p) basis set[93–97]], at the RB3LYP-D3(BJ)/def2-TZVP optimised geometry of each molecule investigated in this paper. NICS values and volume data needed for T_1 isotropic shielding isosurfaces were obtained in a similar way, using UB3LYP-GIAO/6-311++G(d,p) calculations at UB3LYP-D3(BJ)/def2-TZVP geometries. In all volume data calculations, $\sigma_{iso}(\mathbf{r})$ was evaluated on regular three-dimensional grids of points with a spacing of 0.1 Å. To reduce computational effort, shielding tensors were calculated at the symmetry-unique points (using Abelian symmetry only) and then data was replicated via symmetry to create a complete grid. To enable visualisation, all $\sigma_{iso}(\mathbf{r})$ values from the RB3LYP-GIAO/6-311++G(d,p) and UB3LYP-GIAO/6-311++G(d,p) calculations for each molecule were assembled in GAUSSIAN cube files.

In line with previous work on NICS and ring currents in triplet systems (see, for example, refs. [98] and [99]), the UB3LYP-GIAO magnetic properties of the T_1 states of compounds with condensed thiophene rings computed in this paper include the contributions arising from the perturbation to the Kohn-Sham orbitals only. The omission of the large terms associated with the interaction of the electronic spin angular momentum and the magnetic field[100,101] means that the reported numbers will exhibit considerable differences from experimental measurements when and if such measurements become available. The advantage of the approach adopted here is that the values reported for triplet states can be compared directly to those for singlet states.

All geometry optimisations, analytical harmonic frequency and shielding calculations reported in this paper were carried out in the gas phase and were performed using GAUSSIAN.[102] All optimised geometries, additional computational details and the GAUSSIAN cube files with shielding data are included in the Supporting Information. The $\sigma_{iso}(\mathbf{r})$ volume data provided in the GAUSSIAN cube files allow inspection of a number of aspects of the shielding distributions around the S_0 and T_1 states of the molecules we investigated, including construction of shielding isosurfaces at different $\sigma_{iso}(\mathbf{r})$ values, $\sigma_{iso}(\mathbf{r})$ contour plots in various planes and $\sigma_{iso}(\mathbf{r})$ scans along selected directions. Values of the HOMA and Bird indices were computed using Multiwfn.[103]

Results and Discussion

Thiophene

Our S_0 NICS(0) and NICS(1) values for thiophene of −13.0 and −10.4 ppm, respectively (Table 1), are close to the RB3LYP-GIAO/6-311+G(d,p)//RB3LYP/6-311+G(d,p) values of −12.9 and −10.2 ppm reported by Schleyer and co-workers,[104] as well as to the RHF-GIAO/6-311++G(d,p) and RMP2-GIAO/6-311++G(d,p) (restricted Hartree-Fock and second-order Møller-Plesset perturbation theory utilizing GIAOs) NICS(0) and NICS(1) values calculated at the experimental gas-phase geometry of thiophene,[16] and confirm, as expected, that in its electronic ground state this molecule shows a level of aromaticity similar

Table 1. NICS(0) and NICS(1) values for the symmetry-unique rings in the S_0 and T_1 electronic states of **1**–**12** (in ppm). For planar geometries, NICS(−1)= NICS(+1). For further details, see text.

Ring	S_0 NICS(0)	S_0 NICS(−1)	S_0 NICS(+1)	T_1 NICS(0)	T_1 NICS(−1)	T_1 NICS(+1)
1a	−13.0	−10.4	−10.4	4.3	3.7	5.1
2a	−11.0	−8.8	−8.8	35.2	30.2	30.3
3a	−11.2	−8.9	−8.9	5.4	5.5	5.5
4a	−7.2	−6.2	−6.2	−3.6	−2.8	−2.8
4b	−13.5	−10.8	−10.8	7.8	7.3	7.3
5a	−12.7	−11.3	−11.3	−0.6	−0.3	−0.3
6a	−11.3	−8.7	−8.7	12.2	12.4	12.8
6b	−8.9	−7.0	−7.0	41.9	34.5	34.5
7a	−11.3	−8.5	−8.5	0.5	1.5	1.5
7b	−9.4	−7.4	−7.4	4.6	4.7	4.7
8a	0.8	−6.9	3.0	−12.9	−20.7	−5.6
8b	−7.0	−7.2	−2.6	−9.1	−12.1	−3.2
8c	–	–	–	−6.2	−9.7	−1.3
9a	6.7	−0.3	4.3	3.5	−2.4	2
9b	−8.6	−7.8	−4.7	−0.6	1.4	3.3
9c	–	–	–	−5.6	−4.5	−2.5
9d	–	–	–	−10.1	−8.6	−5.5
9e	–	–	–	−12.5	−10.6	−7.0
10a	5.4	2.6	2.6	4.1	2.6	2.7
10b	−9.7	−6.9	−6.9	14.1	14.3	15.8
10c	–	–	–	8.3	9.7	10.7
11a	4.8	3.0	3.0	1.5	0.3	0.4
11b	−9.3	−6.5	−6.5	8.9	9.0	9.7
11c	–	–	–	−4.0	−2.2	−1.8
11d	–	–	–	−9.3	−6.6	−6.6
11e	–	–	–	−9.5	−6.8	−6.7
11f	–	–	–	−10.1	−7.5	−7.3
12a	4.7	3.1	3.1	3.7	2.1	2.3
12b	−9.0	−6.4	−5.8	−1.4	1.3	2.1
12c	−9.0	−6.4	−5.8	−0.6	1.5	−0.1
12d	−8.8	−6.5	−5.5	−8.1	−6.2	−4.8
12e	−9.1	−6.2	−6.2	−9.1	−6.8	−6.1
12f	−8.8	−6.5	−5.5	−9.3	−7.0	−6.0
12g	–	–	–	−8.5	−6.8	−4.9

to that of benzene. Our T_1 NICS(0), NICS(+1) and NICS(−1) values at the T_1 optimised geometry of 4.3, 3.7 and 5.1 ppm, respectively, indicate that thiophene experiences a Baird-style aromaticity reversal between S_0 and T_1. However, the magnitude of this S_0–T_1 aromaticity reversal appears to be much lower than that reported for benzene: The S_0 NICS(0) and NICS(1) values for benzene, −8.2 and −9.5 ppm, respectively, change to 39.6 and 30.1 ppm, respectively in T_1; these S_0 and T_1 values were calculated with CASSCF(6,6)-GIAO/6-311++G-(2d,2p) wavefunctions (π space complete-active-space self-consistent field with '6 electrons in 6 orbitals' and GIAOs), for a vertical excitation at the experimental electronic ground state geometry.[105] For comparison purposes, we also calculated the NICS(0) and NICS(1) values for the T_1 state of thiophene at the S_0 optimised geometry, that is, for a vertical excitation. This produced much higher NICS(0) and NICS(1) T_1 values of 28.4 and 24.7 ppm, respectively, which are closer to but still noticeably lower than those for the T_1 state of benzene. It has been observed on the examples of naphthalene and anthracene[106] that, when used to calculate magnetic properties, UB3LYP-GIAO overestimates the antiaromaticity of the T_1 state in comparison to CASSCF-GIAO and a switch to a CASSCF-GIAO description of this state in thiophene (and in the other thiophene-based compounds studied in this paper) is likely to detect a lower level of antiaromaticity. This is an indication that, whereas the levels of aromaticity of the S_0 states of benzene and thiophene are comparable, the T_1 state of benzene is more antiaromatic than the T_1 state of thiophene. The very significant difference between the NICS(0) and NICS(1) values for the T_1 state of thiophene at the S_0 optimised geometry, and the NICS(0) and NICS(1) values at the T_1 optimised geometry shows the extent to which the T_1 geometry optimisation allows the molecule to adapt to the antiaromatic character of this state and decrease its level of antiaromaticity. For molecules containing two or more condensed thiophene rings we examine the magnetic properties of the respective T_1 states at T_1 optimised geometries only – the reason for doing so is that, for some of these molecules, the 'triplet' UB3LYP Kohn-Sham determinant at the S_0 geometry turns out to be of 'broken-symmetry', that is, of spatial symmetry lower than that of the nuclear framework, which leads to unphysical results for the nuclear and off-nucleus shielding tensors.

The $\sigma_{iso}(\mathbf{r})$ isosurface plots for the S_0 and T_1 states of thiophene at the respective optimised geometries are shown in Figure 2. The isovalues of $\sigma_{iso}(\mathbf{r}) = \pm 16$ ppm were chosen so as to provide optimal levels of detail; the same isovalues are used in all figures displaying $\sigma_{iso}(\mathbf{r})$ isosurfaces in this paper. Isosurfaces for other isovalues can be inspected using the GAUSSIAN cube files provided in the Supporting Information. As can be seen in Figure 2, in the electronic ground state the five-membered ring is very well-shielded, even slightly more so than the six-membered ring in benzene,[107,108] which is due mostly to placing the same number of π electrons in a ring of a smaller size. This observation is in line with the $\sigma_{iso}(\mathbf{r})$ contour plots for the electronic ground state of thiophene constructed from shielding data calculated at the RMP2-GIAO/6-311++G(d,p) level[16] and confirms the presence of strong bonding

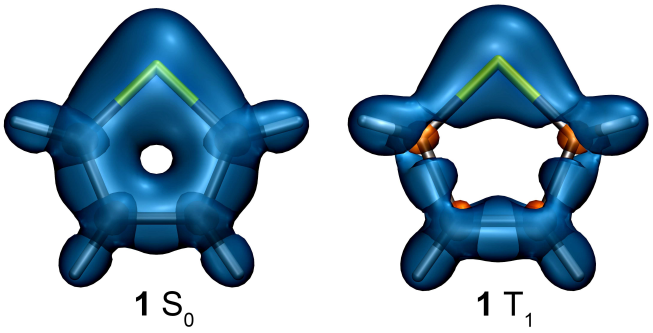

Figure 2. Shielding around the S_0 and T_1 states of thiophene **1**. Isosurfaces at $\sigma_{iso}(\mathbf{r}) = +16$ ppm (shielded regions, blue) and $\sigma_{iso}(\mathbf{r}) = -16$ ppm (de-shielded regions, orange).

interactions and aromatic stability. By comparison, in the T_1 state of thiophene (Figure 2) the five-membered ring is considerably less shielded, which is a clear indication of a marked decrease in aromaticity. However, the absence of a strongly deshielded central region similar to that present in the electronic ground state of cyclobutadiene (see, for example, ref. [21]) makes it difficult to argue in favour of sizeable antiaromatic character.

The differences between the S_0 and T_1 optimised geometries of thiophene are considerable: In addition to the reduction in symmetry (see above), the S–C_1, C_1–C_2 and C_2–C_2 bond lengths (C_1 and C_2 stand for the two symmetry-unique carbon atoms, C_1 is adjacent to S) change from 1.718, 1.365 and 1.422 Å in S_0 to 1.771, 1.463 and 1.343 Å in T_1, respectively, that is, the C_1–C_2 'double' bonds in S_0 become 'single' bonds in T_1 and the C_2–C_2 'single' bond in S_0 becomes a 'double' bond in T_1. These differences are reflected in the decreased shielding over the S–C_1 and C_1–C_2 bonds in T_1 in comparison to S_0 (Figure 2); the C_2–C_2 bond is more shielded than the C_1–C_2 bonds in T_1 but it is less shielded than in S_0. The last observation suggests that the levels of shielding over corresponding bonds in electronic states that exhibit different levels of antiaromaticity may not reflect correctly the respective differences in bond strength and length – the reason for this is that the presence of a central deshielded region in an antiaromatic ring can cause exaggerated deshielding of the bonds in that ring.

The carbon atoms in the S_0 and T_1 electronic states of thiophene and all other thiophene-based compounds studied in this paper are surrounded by small ovoid deshielded regions inside which $\sigma_{iso}(\mathbf{r})$ becomes negative. These regions are more noticeable in the $\sigma_{iso}(\mathbf{r})$ isosurface plots for the T_1 states in which the carbon-carbon and carbon-sulfur bonds are less shielded. Similar deshielded 'halos' around sp^2 and sp hybridized carbon atoms and other sp^2 hybridized first main row atoms have been observed previously in conjugated rings,[16,107,108] as well as in open-chain conjugated molecules such as ethene, ethyne and *s-trans*-1,3-butadiene.[109,110] The presence of deshielded 'halos' around the carbon atoms in all $\sigma_{iso}(\mathbf{r})$ isosurface plots reported in this paper suggests that the hybridisation states of these atoms are close to sp^2; there are no such 'halos' around the sulfur atoms. The close to sp^2 hybridisation states of the carbon

atoms suggests that referring to the Kohn-Sham orbitals in the non-planar thiophene-based compounds examined in this paper as (almost) σ and π orbitals can be viewed as a reasonable approximation; this approximation is also supported by comparisons between the shapes of these orbitals throughout the series **1–12**.

Thienothiophenes

According to the NICS values that we obtained, all thiophene rings in the electronic ground states of the four thienothiophenes studied in this paper (**2**–**5** in Figure 1) are aromatic, with NICS(0) values between −13.5 and −7.2 ppm, and NICS(1) values between −11.3 and −6.2 ppm (Table 1). These results show that the positions of the sulfur atoms within the two condensed thiophene rings can influence significantly the respective NICS values and levels of aromaticity – for example, the NICS(0) values for the two thiophene rings in the asymmetric thieno[3,4-*b*]thiophene **4** show a considerable difference, −7.2 and −13.5 ppm for rings **4a** and **4b**, respectively. The different levels of aromaticity of these rings are well-illustrated by the $\sigma_{iso}(\mathbf{r})$ isosurface plot in Figure 3: While the carbon-carbon and carbon-sulfur bonds in both rings are well-shielded, the shielding 'hole' in the centre of ring **4a** (on the left) is much larger than that in the centre of ring **4b** (on the right). The most shielded thiophene rings within the thienothiophenes **2**–**5** are rings **4b** and **5a**, in which the sulfur atoms are positioned similarly; the higher levels of shielding are in correspondence with the respective NICS values. This shielding behaviour can be attributed to the shorter carbon-sulfur bond lengths in rings **4b** and **5a** in comparison to the respective bond lengths in rings **2a**, **3a** and **4a** (for both of **4b** and **5a**, it is possible to draw resonance stuctures in which the sulfur atom is engaged in two 'double' bonds; one of these structures for **5a** is shown in Figure 1). The shorter carbon-sulfur bond lengths allow the two electrons contributed by each sulfur atom to engage more fully in the π systems of rings **4b** and **5a**. As a consequence, the local aromaticities of rings **4b** and **5a** estimated using magnetic shielding criteria are out of line with the ordering of the energies of the S_0 optimised geometries of the four thienothiophenes (see the Supporting Information). According to our results, the lowest-energy thienothiophene is **3**, closely followed by **2**; the energy gaps between **2** and **4**, and between **4** and **5** are larger. The energy ordering of **2**, **3** and **4** is supported by the NICS values in Table 1, if we compare the NICS values for rings **2a** and **3a** to the average NICS values for rings **4a** and **4b** (the lower shielding over ring **4a** compensates for the higher shielding over ring **4b**). However, the thiophene rings **5a** in the least stable thienothiophene, thieno[3,4-*c*]thiophene **5**, turn out to be more shielded and to have more negative NICS values than rings **2a** and **3a**.

Overall, the S_0 shielding isosurfaces for the other two thienothiophenes (**2** and **3**, Figure 3) are very similar to the outcomes that would be expected from fusing together the S_0 isosurfaces for two thiophene rings over the shared carbon-carbon bond. In general, the geometries of the individual thiophene rings in the S_0 optimised geometries of **2**–**5** retain some features of the S_0 geometry of thiophene such as the positions of the carbon-carbon 'single' and 'double' bonds. Similar observations can be made for the S_0 optimised geometries of the remaining compounds with fused thiophene rings studied in this paper, **6**–**12**.

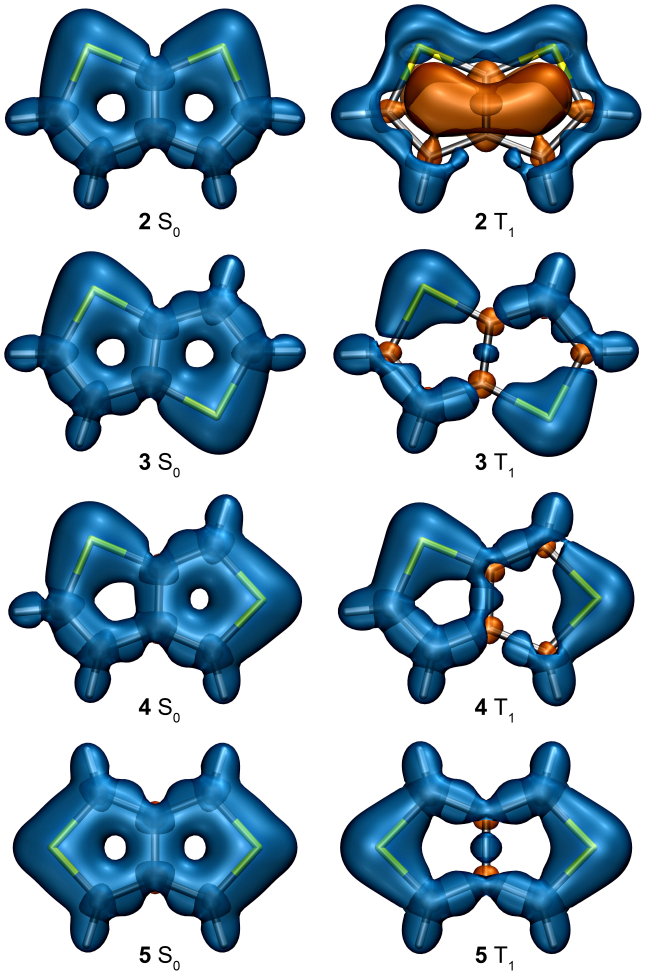

Figure 3. Shielding around the S_0 and T_1 states of thieno[2,3-*b*]thiophene **2**, thieno[3,2-*b*]thiophene **3**, thieno[3,4-*b*]thiophene **4** and thieno[3,4-*c*]thiophene **5**. Isosurface details as for Figure 2.

The differences between the aromatic properties of the T_1 states of the four thienothiophenes are more pronounced, as illustrated by the respective shielding isosurfaces (Figure 3). The only well-defined Baird-style aromaticity reversal from a distinctly aromatic S_0 state to a distinctly antiaromatic T_1 state is observed for thieno[2,3-*b*]thiophene **2**. The antiaromaticity of the T_1 state of this molecule is associated with the presence of a large strongly deshielded central region outlined by the $\sigma_{iso}(\mathbf{r}) = -16$ ppm isosurface, the shape of which resembles a combination of two dumbbells, one inside each ring, interconnected over the fused carbon-carbon bond. This strongly deshielded region leads to a noticeable reduction of shielding over the peripheral carbon-carbon and carbon-sulfur bonds, in comparison to the shielding picture in S_0, and to a displacement

of this shielding toward the exteriors of the rings; there is very little if any shielding over the fusion bond. The high antiaromaticity of this T_1 state is emphasized by the NICS(0), NICS(+1) and NICS(−1) values of 35.2, 30.2 and 30.3 ppm, respectively, for the symmetry-equivalent thiophene rings **2a**. Despite the molecular symmetry reduction on switching from S_0 to T_1 (C_{2h} to C_2), the associated changes in the central region of the geometry of the carbon-sulfur skeleton of thieno[2,3-*b*]thiophene **2** are relatively minor; as a result, the off-nucleus shielding picture in T_1 is very similar to those observed for S_0 to T_1 vertical excitations in naphthalene and anthracene,[106] and shows a high level of antiaromaticity. It should be noted that despite the complete deshielding of the fusion bond in the T_1 state, its length in the optimised geometry of this state is not much longer than that in the S_0 optimised geometry, 1.405 against 1.392 Å. Just as in the case of thiophene, this observation can be associated with the strongly deshielded central region which causes exaggerated deshielding of all bonds and, especially, of the fusion bond. In general, the bonds in the T_1 states of **3–5** are less deshielded than those in the T_1 state of **2**, and the respective shielding pictures have more in common with that for the T_1 state of thiophene.

The changes in the off-nucleus shielding distributions and hence aromaticity levels of the remaining three thienothiophenes on passing from S_0 to T_1 are less pronounced (compare the isosurfaces for **3–5** in Figure 3) and similar to the corresponding change observed in thiophene (Figure 2). The thiophene rings in the T_1 states of **3–5** (Figure 3) can be separated into two groups according to the behaviour of $\sigma_{iso}(\mathbf{r})$ in and around these rings. These groups of less and more shielded rings include rings **3a** and **4b**, and rings **4a** and **5a**, respectively. The T_1 NICS(0) and NICS(1) values for ring **3a** are 5.4 and 5.5 ppm, respectively, and the corresponding values for ring **4b** are 7.8 and 7.3 ppm, respectively (see Table 1). While these NICS values are positive, they are not sufficiently high to imply other than borderline levels of antiaromaticity. The T_1 NICS(0) and NICS(±1) values for rings **4a** and **5a** are negative, −3.6 and −2.8 ppm, respectively, for ring **4a**, and −0.6 and −0.3 ppm, respectively, for ring **5a**. Both sets of values indicate that these two rings are mostly non-aromatic. The partial deshielding of the fusion bonds in the T_1 states of thieno[3,2-*b*]thiophene **3**, thieno[3,4-*b*]thiophene **4** and thieno[3,4-*c*]thiophene **5** (Figure 3) suggests a close to evenly balanced competition between aromatic and antiaromatic behaviours. Overall, according to the NICS values and the variations in the off-nucleus shielding, the T_1 states of these three thienothiophenes should be considered as non-aromatic.

The $\sigma_{iso}(\mathbf{r})$ isosurfaces and NICS values obtained for compounds **2–5** show clearly that the way in which two thiophene rings are fused together has a significant impact on aromaticity and bonding in the S_0 and T_1 states of the resulting thienothiophene.

Looking at the positions of the carbon-carbon 'single' and 'double' bonds, the geometries of the individual thiophene rings in the T_1 optimised geometry of **2** are intermediate between the S_0 and T_1 geometries of thiophene, with relatively minor changes in the central region indicating a tendency towards bond equalisation, while those of the individual thiophene rings in the T_1 optimised geometry of **3** are closer to the T_1 geometry of thiophene. This is in line with the observation that the changes in the magnetic shielding picture between the S_0 and T_1 states of **2** resemble those expected for a vertical excitation (see above), while the corresponding changes for **4** resemble those for a thiophene molecule shown in Figure 2. The main changes between the S_0 and T_1 geometries of **4** and **5** are in the rings containing a sulfur atom engaged in two 'double' bonds in the S_0 state; the carbon-sulfur bond lengths involving this atom become much longer in the T_1 state which contributes to the deshielding of the interiors of the corresponding rings.

Dithienothiophenes

The S_0 shielding isosurfaces for dithieno[2,3-*b*:3′,2′-*d*]thiophene **6** and dithieno[3,2-*b*;2′,3′-*d*]thiophene **7** (Figure 4) continue the trend observed in the corresponding shielding isosurfaces for their precursors, thieno[2,3-*b*]thiophene **2** and thieno[3,2-*b*]thiophene **3** (Figure 3) and look very similar to the outcomes that would be expected from fusing together the S_0 isosurfaces for three thiophene rings over the shared carbon-carbon bonds. All three thiophene rings in both molecules are well-shielded which indicates that each of these rings is aromatic.

On switching states from S_0 to T_1, the central ring **6b** in **6** becomes strongly antiaromatic, as shown by the extensive deshielding of the interior of the ring and of the carbon-carbon bonds fusing it to the adjacent **6a** rings. With its NICS(0) value of 41.9 ppm and NICS(+1) = NICS(−1) values of 34.5 ppm, ring **6b** turns out to be the most antiaromatic thiophene ring amongst the T_1 states of all thiophene-based compounds studied in this paper. The peripheral **6a** rings are less deshielded but, with NICS(0), NICS(+1) and NICS(−1) values of 12.2, 12.4 and 12.8 ppm, respectively, these rings are also antiaromatic. Dithieno[2,3-*b*:3′,2′-*d*]thiophene **6** and its precursor, thieno[2,3-*b*]thiophene **2**, share the orientations of the

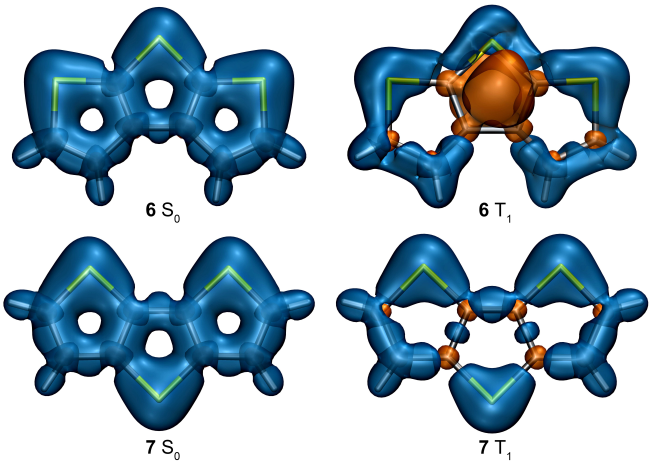

Figure 4. Shielding around the S_0 and T_1 states of dithieno[2,3-*b*:3′,2′-*d*]thiophene **6** and dithieno[3,2-*b*;2′,3′-*d*]thiophene **7**. Isosurface details as for Figure 2.

fused thiophene rings observed in the sulflowers **8–12**. Our results show that both of **2** and **6** are definitely Hückel-aromatic in their S_0 states and Baird-antiaromatic in their T_1 states. It is reasonable to expect that the S_0 and T_1 states of the next two members of this series, with four and five thiophene rings, respectively, thieno[3′,2′:4,5]thieno[2,3-*b*]thieno[3,2-*d*]thiophene and thieno[3′,2′:4,5]thieno[2,3-*b*]thieno[3′,2′:4,5]thieno[3,2-*d*]thiophene, will behave similarly; however, it would be premature to make analogous assumptions about sulflowers (see below).

While the different orientations of the thiophene rings in **6** and **7** do not lead to noticeable differences between the aromaticities of the respective electronic ground states, the T_1 state of **7** is significantly less antiaromatic than the T_1 state of **6**. This is demonstrated by the much lower levels of deshielding of the interiors of rings **7a** and **7b** as opposed to those of rings **6a** and **6b** (compare the corresponding isosurfaces in Figure 4) and the much lower T_1 NICS(0) and NICS(1) values of 0.5 and 1.5 ppm for ring **7a**, and 4.6 and 4.7 ppm for ring **7b**, respectively. In fact, according to these NICS values the T_1 state of dithieno[3,2-*b*;2′,3′-*d*]thiophene **7** should be classified as mostly nonaromatic.

The comparison of the geometries of the individual thiophene rings in the T_1 optimised geometries of **6** and **7** to the S_0 and T_1 optimised geometries of thiophene shows that the positions of the 'single' and 'double' carbon-carbon bonds in the terminal rings **6a** in the T_1 geometry of **6** match the positions of the corresponding bonds in the T_1 geometry of thiophene, but the bond length alternation pattern in the central ring **6b**, while similar to that in the S_0 geometry of thiophene, is more bond-equalised, with shorter carbon-sulfur bonds and longer carbon-carbon bonds. The positions of the 'single' and 'double' carbon-carbon bonds in all three rings in the T_1 geometry of **7** match the positions of the corresponding bonds in the T_1 geometry of thiophene. The nonplanar geometry of the T_1 state of **6** decreases the conjugation between bonds from different thiophene rings and helps enhance the local traits in the electronic structure; together with the bond alternation pattern in the central ring in **6** this feature makes the deshielding of this central ring more pronounced, as in the case of a vertical excitation.

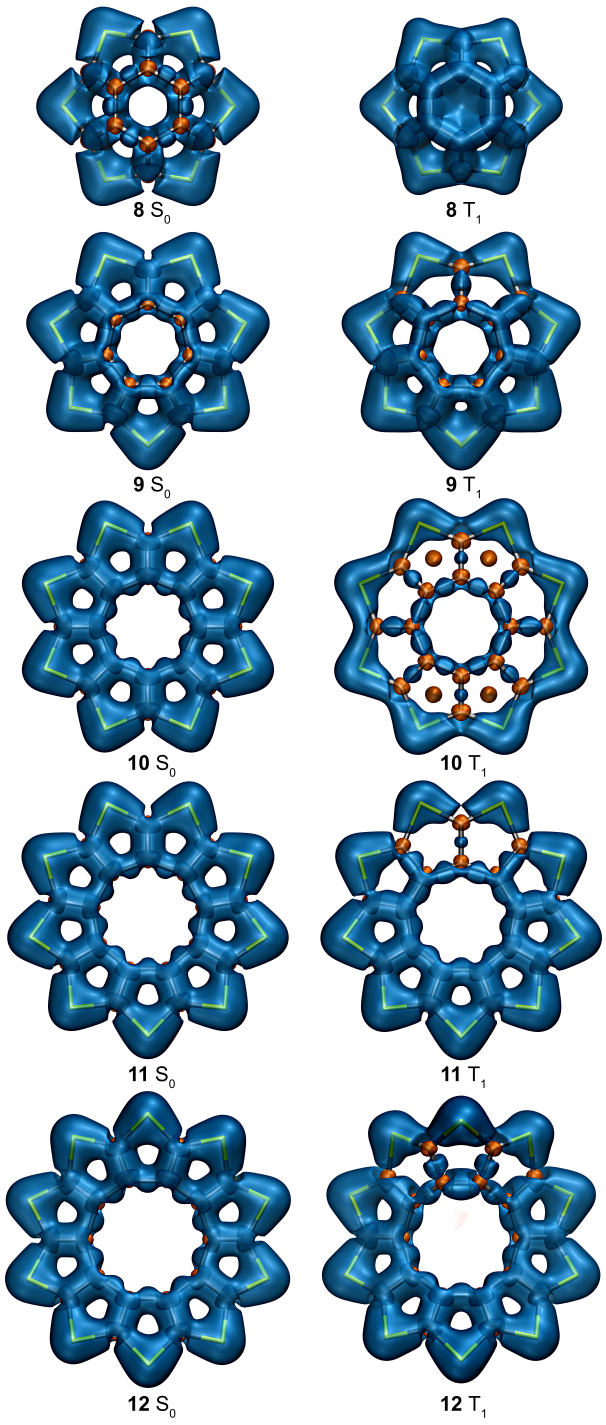

Figure 5. Shielding around the S_0 and T_1 states of sulflowers with six **8**, seven **9**, eight **10**, nine **11** and ten **12** thiophene rings. Views from top for bowl-shaped geometries. Isosurface details as for Figure 2.

Sulflowers

The S_0 shielding isosurfaces for $(C_2S)_6$–$(C_2S)_{10}$ (**8–12**) shown in Figure 5 suggest that the electronic ground states of these sulflowers are aromatic: Each individual thiophene ring is well-shielded, similarly to those in thieno[2,3-*b*]thiophene **2** (Figure 3) and dithieno[2,3-*b*:3′,2′-*d*]thiophene **6** (Figure 4), which implies that the fusion of thiophene rings to form a sulflower preserves the aromaticities of these rings and produces an aromatic molecule.

The shielding over the carbon-carbon and carbon-sulfur bonds in the S_0 state of $(C_2S)_6$ is predominantly inside the bowl; there is noticeably less shielding over these bonds outside the bowl. This is an indication that the thiophene rings in $(C_2S)_6$ are less aromatic than their counterparts in $(C_2S)_7$–$(C_2S)_{10}$ which is most likely due to stronger ring strain resulting in a deeper bowl and less electron presence and shielding activity outside the bowl. Ring strain in the S_0 optimised geometries of the series $(C_2S)_6$–$(C_2S)_{10}$ initially decreases, through the bowl-shaped $(C_2S)_6$ **8** and $(C_2S)_7$ **9**, to the planar $(C_2S)_8$ **10** and $(C_2S)_9$ **11**, and then increases again to produce the corrugated-shape $(C_2S)_{10}$

12 (see below). Despite these variations in ring strain, the differences between the shielding over corresponding carbon-carbon and carbon-sulfur bonds in **9**–**12** in their electronic ground states are relatively minor and difficult to distinguish visually. Each of the S_0 shielding distributions for **8**–**12** includes a relatively small deshielded region around the centre of the respective 'inner' ring (rings **8a**, **9a**, **10a**, **11a** and **12a**); these regions can be examined in detail using the GAUSSIAN cube files included in the Supporting Information. The sizes of the deshielded regions and the levels of deshielding suggest that none of the 'inner' rings in the S_0 states of **8**–**12** show more than borderline levels of antiaromaticity and that it might be more appropriate to consider all of these 'inner' rings as nonaromatic; however, the presence of these regions is a feature which cannot be explained using simple electron-counting rules.

It is instructive to juxtapose the S_0 NICS values for the 'inner' rings in **8**–**12** with the corresponding values for benzene (D_{6h} symmetry), NICS(0) = −8.0 ppm and NICS(1) = −10.2 ppm, and rectangular cyclobutadiene (D_{2h} symmetry), NICS(0) = 26.3 ppm and NICS(1) = 17.3 ppm, calculated at exactly the same level of theory as the one used in the current work.[21] It should be noted that rectangular cyclobutadiene is considerably less antiaromatic than square cyclobutadiene (D_{4h} symmetry).[105] While this is not meant to suggest that NICS values provide a strictly linear aromaticity scale, we observe that all NICS(0), NICS(−1) and NICS(+1) values for the 'inner' rings in **8**–**12** (Table 1) are either below or very close to the averages of the NICS(0) and NICS(1) values for benzene and rectangular cyclobutadiene, ca. 9.2 and 3.6 ppm, respectively, which confirms the predominantly nonaromatic character of these rings.

The comparison between the S_0 NICS(0), NICS(+1) and NICS(−1) values for rings **8b**, **9b**, **10b**, **11b** and **12b**–**12f** (see Table 1), and their counterparts for thiophene shows that each of the fused rings in the respective sulflower is less aromatic than thiophene itself. According to the NICS data, the aromaticity of the individual thiophene rings initially increases between **8** and **10**, and then decreases between **10** and **12**.

The logic behind our conclusion that the S_0 states of **8**–**12** are aromatic is that the fusion of 6–10 locally aromatic thiophene rings and the establishment of a mostly nonaromatic 'inner' ring should produce a globally aromatic molecule. On the basis of examining the net magnetically induced current strengths (the sums of the magnetically induced current strengths along the 'inner' and 'outer' rings), Karaush-Karmazin and co-authors,[24] who studied the electronic ground states of a wider range of sulflowers, $(C_2S)_5$–$(C_2S)_{12}$, assert that $(C_2S)_5$–$(C_2S)_7$ are antiaromatic, $(C_2S)_8$–$(C_2S)_{10}$ are mostly nonaromatic, and the more strained nonplanar $(C_2S)_{11}$ and $(C_2S)_{12}$ are aromatic, despite reporting NICS(0) values for the thiophene rings in $(C_2S)_6$–$(C_2S)_{10}$ and a NICS(1) value for ring **10b** which are reasonably close to those obtained in the current work and acknowledging that these thiophene rings are locally aromatic. It should be noted that we obtained a local minimum of D_{9h} symmetry for the electronic ground state of $(C_2S)_9$, but the data reported in ref. [24] suggests that the planar $(C_2S)_9$ geometry used in that paper is of a lower C_{2v} symmetry – this difference is most likely due to the inclusion of empirical dispersion corrections and the use of a larger basis set in the current work. The ring currents from two adjacent rings in a sulflower $(C_2S)_n$ of D_{nv} or C_{nv} symmetry cancel or nearly cancel along the spoke bond fusing these rings. Magnetically induced currents can be integrated to produce shielding tensors by means of the Biot-Savart law (see, for example, ref. [111]), and the expectation is that no or next to no current density along the spoke bonds would result in low levels of magnetic shielding over these bonds. However, the S_0 shielding isosurfaces for $(C_2S)_6$–$(C_2S)_{10}$ (**8**–**12**) shown in Figure 5 demonstrate that all spoke bonds in these sulflowers are well-shielded; a very similar discrepancy between ring currents and shielding over spoke bonds is observed in coronene and corrannulene.[112] These observations suggest that magnetically induced currents do not account properly for the local aromaticities of the individual thiophene rings in sulflowers, and of the individual benzene rings in coronene and corrannulene. As a consequence, the predictions about the aromaticities of fused compounds of this type made on the basis of magnetically induced ring currents can be questionable and contradictory to chemical intuition.

At first glance, the changes in the shapes of the shielding isosurfaces for **8**–**12** on passing from S_0 to T_1 are anything but uniform. As shown in Figure 5, the carbon-carbon and carbon-sulfur bonds and the interior of the 'inner' ring in the smallest sulflower we investigated, $(C_2S)_6$ **8**, are noticeably more shielded in T_1 than in S_0, which is a clear indication of a higher level of aromaticity. This observation is supported by the T_1 NICS(0) and NICS(−1) values for rings **8b** and **8c**, −9.1 and −6.2 ppm, and −12.1 and −9.7 ppm, respectively (Table 1). The T_1 NICS(+1) values for both types of ring calculated outside the bowl are smaller in magnitude and fall within the nonaromatic region. In addition, in the T_1 state $(C_2S)_6$ no longer features a deshielded region around the centre of its 'inner' ring; in fact, this ring (**8a**) is characterized by T_1 NICS(0), NICS(−1) and NICS(+1) values of −12.9, −20.7 and −5.6 ppm (see Table 1), the first two of which suggest strong aromaticity. In contrast, the shielding distributions in the S_0 and T_1 states or $(C_2S)_7$ **9** show fewer differences – in S_0, all symmetry-equivalent thiophene rings are equally shielded, and in T_1 three thiophene rings (**9d** and **9e**) are more shielded than their counterparts in S_0, two further thiophene rings (**9c**) are shielded slightly less than in S_0, and the remaining two thiophene rings (**9b**) are noticeably less shielded than in S_0. Shielding in and around the 'inner' ring **9a** in T_1 remains much the same as in S_0, and the deshielded central region from S_0, in which shielding goes down to −4 ppm, is still present in T_1. These observations suggest that $(C_2S)_7$ **9** experiences next to no change in aromaticity on passing from S_0 to T_1 and are supported by the S_0 and T_1 NICS(0), NICS(−1) and NICS(+1) values for rings **9a**–**9e** included in Table 1.

The addition of a further thiophene ring in the next member of the sulflower series, $(C_2S)_8$ **10**, leads to a marked change in the shielding distribution characterizing the T_1 state: All eight thiophene rings become antiaromatic, with deshielded regions above and below the centre of each ring and mostly inside the bowl; in four of these deshielded regions (these can be observed within rings **10b**, see Figure 5) $\sigma_{iso}(\mathbf{r})$ goes down to ca.

−20 ppm; in the remaining four rings **10c** it goes down to ca. −13 ppm. The positions at which the T_1 NICS(0) and NICS(1) values are calculated for rings **10b** and **10c** are not the most deshielded locations within the deshielded regions in these rings (Table 1); however, the positive NICS values which go up to 15.8 pm for NICS(−1) in rings **10b** support the conclusion that **10** is antiaromatic in its T_1 state. Shielding around the 'inner' ring **10a** is weakened in comparison to S_0; similarly to S_0, there is a deshielded region close to the centre of this ring, at which NICS(0) = 4.1 ppm.

The signs of antiaromaticity in the T_1 state of $(C_2S)_9$ **11** are much fewer: Just the two symmetry-equivalent adjacent thiophene rings **11b** feature deshielded regions close to their centres, with $\sigma_{iso}(\mathbf{r})$ reaching close to −11 ppm, and two further rings, **11c** are less shielded than their counterpart, **11b**, in S_0. However, the remaining five thiophene rings, **11d**–**11f** appear to be just as well shielded as **11b** in S_0. The T_1 NICS(0) and NICS(1) values for rings **11d**–**11f** (Table 1) indicate that rings **11d** and **11e** are just as aromatic in T_1 as ring **11e** is in S_0, while ring **11f** is more aromatic in T_1 than ring **11e** is in S_0. All in all, the T_1 state of $(C_2S)_9$ **11** combines two antiaromatic, two nonaromatic and five aromatic thiophene rings; the 'inner' ring features a small deshielded region near its centre, but the levels of deshielding and the associated NICS values indicate that this ring should be considered as nonaromatic.

The shielding isosurfaces and the NICS values for the T_1 state of **12** suggests that none of the ten thiophene rings are antiaromatic; three thiophene rings, **12b** and **12c**, show some deshielding and lower NICS values in comparison the thiophene rings in S_0, while the shielding around each of the remaining seven thiophene rings and the respective NICS values are very similar to those for the thiophene rings in S_0. These observations indicate that the T_1 state of **12** involves three nonaromatic and seven aromatic thiophene rings. Shielding around the 'inner' ring **12a** is similar to that in S_0; just as in S_0, there is a deshielded region close to the centre of this ring, at which NICS(0) = 3.7 ppm, 1 ppm lower than in S_0, and so in T_1 this ring remains nonaromatic.

Our results show that the smaller sulflowers $(C_2S)_6$ **8** and $(C_2S)_7$ **9** are 'reluctant' to become antiaromatic in T_1; in the larger sulflowers $(C_2S)_9$ **11** and $(C_2S)_{10}$ **12** T_1 antiaromaticity is limited to a small number of thiophene rings. The most well-defined aromaticity reversal between S_0 and T_1 in the series **8**–**12** is observed in $(C_2S)_8$ **10** – the most aromatic sulflower in S_0 becomes the most antiaromatic one in T_1.

The unexpected increase of the aromaticity of $(C_2S)_6$ **8** on passing from the S_0 to the T_1 state is supported by the comparison between the optimised geometries of the two states. As a consequence of its C_{6v} symmetry, the S_0 geometry has only three symmetry-unique bond lenghts, those of the carbon-sulfur rim (outer ring), and of carbon-carbon spoke and hub (inner ring) bonds, measuring 1.780, 1.367 and 1.424 Å, respectively. The lower C_{2v} symmetry of the T_1 state leads to three unique carbon-sulfur rim bond lengths of 1.785, 1.784 and 1.751 Å (there are four bonds of each length), two unique spoke bond lengths of 1.400 (four bonds) and 1.381 Å (two bonds), and two unique hub bond lengths of 1.426 (four bonds) and 1.406 Å (two bonds). Clearly, the combined lengths of the bonds forming the 'outer' and 'inner' rings decrease in the T_1 state; in addition, the individual thiophene rings in this state feature a higher degree of bond equalisation in comparison to their counterparts in the S_0 state. These observations are in line with the increase of the shielding over all bonds on passing from S_0 to T_1 (compare the corresponding isosurfaces for **8** in Figure 5). The T_1 optimised geometry of $(C_2S)_7$ **9** suggests a combination of nonaromatic and aromatic features consistent with the shielding picture in Figure 5. The weakly shielded spoke bond fusing the two **9b** rings is very much a carbon-carbon 'single' bond with a length of 1.475 Å; the better shielded spoke bonds fusing the pairs of **9b** and **9c** rings are significantly shorter, 1.399 Å each, and all remaining spoke bonds have lengths corresponding to carbon-carbon 'double' bonds. Overall, the T_1 geometries of the two thiophene rings **9b** share features of both the S_0 and T_1 geometries of thiophene, and the T_1 geometries of the remaining thiophene rings **9c**–**9e** resemble more the S_0 geometry of thiophene. Because of its C_{2v} symmetry, the T_1 optimised geometry of $(C_2S)_8$ **10** involves two symmetry-unique thiophene rings, **10b** and **10c**. The rings **10b** have geometries intermediate between the S_0 and T_1 geometries of thiophene, with a marked tendency towards carbon-carbon bond equalisation; the geometries of the rings **10c** are closer to the S_0 optimised geometry of thiophene. The longest (and least shielded) carbon-carbon spoke bonds are those between the pairs of rings **10b** – this can be associated with the more pronounced deshielding of the interiors of these rings (Figure 5). The T_1 optimised geometries of $(C_2S)_9$ **11** and $(C_2S)_{10}$ **12** include thiophene rings with geometries which resemble the T_1 geometry of thiophene (**11b** and **12b**), rings with geometries intermediate between the S_0 and T_1 geometries of thiophene (**12c**) and rings with geometries closer to the the S_0 geometry of thiophene (**11c**–**11f** and **12d**–**12g**) which is in line with the shielding pictures in Figure 5.

To analyse ring strain in the S_0 and T_1 electronic states of $(C_2S)_6$–$(C_2S)_{10}$ (**8**–**12**) we followed a procedure analogous to that adopted for the S_0 electronic states of sulflowers in refs. [23] and [24], and calculated the respective energies per C_2S unit,

$$E_{C_2S\ \text{in}\ (C_2S)_n} = \frac{E_{(C_2S)_n}}{n} \quad (1)$$

The $E_{C_2S\ \text{in}\ (C_2S)_n}$ values obtained at the RB3LYP-D3(BJ)/def2-TZVP and UB3LYP-D3(BJ)/def2-TZVP levels, for the S_0 and T_1 electronic states, respectively, are shown in Figure 6 relative to the S_0 and T_1 $E_{C_2S\ \text{in}\ (C_2S)_9}$ values which turned out to be the lowest ones for both states. The changes in ring strain in the S_0 electronic states of $(C_2S)_6$–$(C_2S)_{10}$ are very similar to those reported in refs. [23] and [24], with one difference: At the RB3LYP/6-311++G(d,p) level, the S_0 $E_{C_2S\ \text{in}\ (C_2S)_8}$ value was found to be slightly lower, by 0.2 kcal mol^{-1} than that for $(C_2S)_9$,[24] while our results indicate that the S_0 $E_{C_2S\ \text{in}\ (C_2S)_8}$ value is slightly higher, by just 0.1 kcal mol^{-1} (2.0×10^{-4} a.u.), than that for $(C_2S)_9$.

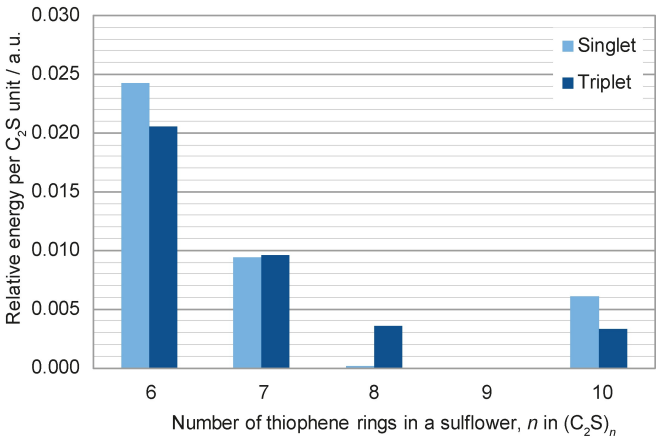

Figure 6. Relative energies per C_2S unit of the S_0 and T_1 electronic states of the sulflowers $(C_2S)_6$–$(C_2S)_{10}$ (**8**–**12**). For further details, see text.

Ring strain in the T_1 electronic states of $(C_2S)_6$–$(C_2S)_{10}$ follows a trend close to that observed in the respective S_0 electronic states: Bowl depth and ring strain decrease from $(C_2S)_6$ to $(C_2S)_8$, $(C_2S)_9$ becomes almost planar and then $(C_2S)_{10}$ assumes a geometry which is significantly more corrugated than the geometry of this sulflower in its ground electronic state. In T_1, the difference between $E_{C_2S\ in\ (C_2S)_8}$ and $E_{C_2S\ in\ (C_2S)_9}$ increases to 2.2 kcal mol^{-1} (3.6×10^{-3} a.u.).

HOMO-LUMO and Singlet-Triplet Gaps

The HOMO-LUMO and singlet-triplet gaps for compounds **1**–**12** are shown in Figure 7. The two types of gap follow rather similar trends (with the exception of thiophene **1**), despite the fact that the singlet-triplet gaps in Figure 7 correspond to the differences between the energies of separately optimised T_1 and S_0 geometries rather than to vertical excitation energies.

Two of the factors influencing the HOMO-LUMO gaps in **1**–**12** are relatively straightforward to account for: These are aromatic stabilisation which increases the HOMO-LUMO gap, and conjugation pathway length which acts in the opposite direction.

The cross-conjugated **2** and **6** feature the largest HOMO-LUMO gaps amongst compounds **2**–**12**. According to our magnetic shielding results, the differences between the S_0 aromaticities of the individual thiophene rings in **2** and **3**, and **6** and **7** are very minor, so that the difference between the HOMO-LUMO gaps in **2** and **3**, and in **6** and **7** can be attributed to the differences between the respective conjugation pathways lengths only. However, **5** which according to our magnetic shielding results involves the most S_0 aromatic thiophene rings amongst **2**–**5** and has conjugation pathways shorter than those in **3** shows the smallest HOMO-LUMO gap amongst the four dithienothiophenes. This is an indication that there are additional important factors influencing the sizes of the HOMO-LUMO gaps which are not that easy to account for qualitatively, for example, the positions of the sulfur atoms.

The HOMO-LUMO gaps of the sulflowers **8**–**12** show better correlation with our magnetic shielding estimates of the S_0 aromaticities of the individual thiophene rings: The HOMO-LUMO gap increases between **8** and **10** and then decreases slightly in **11** and **12**. The corresponding singlet-triplet gaps are in even better agreement with the NICS data in Table 1: The singlet-triplet gaps increase in the sequence **8**–**10** and then noticeably decrease in the sequence **10**–**12**.

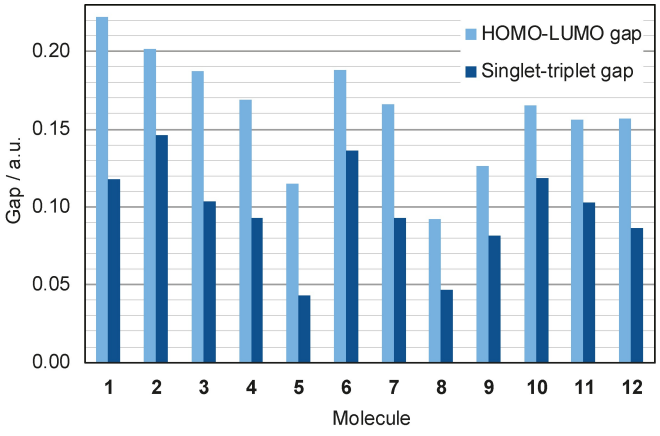

Figure 7. HOMO–LUMO and singlet-triplet gaps for molecules **1**–**12**.

Conclusions

The analysis of the variations of the off-nucleus isotropic magnetic shielding, $\sigma_{iso}(\mathbf{r})$, around thiophene, thienothiophenes, dithienothiophenes and sulflowers in their electronic ground and lowest triplet states, and of the connection between these variations and the geometries of the respective states, reveals that some of the features of aromaticity and bonding in these molecules do not fit in with predictions based on the popular Hückel's and Baird's rules.

Thiophene and the thienothiophenes and dithienothiophenes studied in this paper are systems with $4n+2$ π electron counts of 6, 10 and 14, equal to those of benzene, naphthalene and anthracene, respectively. As expected, the results of the current off-nucleus isotropic magnetic shielding calculations confirm that the electronic ground states of these molecules are aromatic. Similarly to coronene and corannulene, circulenes with 6 and 5 benzene rings, respectively, the fusion of *n* thiophene rings in a sulflower produces a molecule that is aromatic in its electronic ground state, despite having a 4*n* total π electron count, and this is supported by the shielding pictures and NICS values reported in this paper.

Each of the series of compounds with one, two and three fused thiophene rings including thiophene **1**, thieno[2,3-*b*]thiophene **2** and dithieno[2,3-*b*:3′,2′-*d*]thiophene **6**, or thiophene, thieno[3,2-*b*]thiophene **3** and dithieno[3,2-*b*;2′,3′-*d*]thiophene **7**, can be viewed as a thiophene-based heterocyclic analogue of the series comprised of benzene, naphthalene and anthracene. However, our electronic ground state NICS results for these two thiophene-based series of

compounds do not exhibit trends consistent with the set of disputed predictions made on the basis of the NICS values for benzene, naphthalene and anthracene[113,114] known as the 'anthracene problem',[106,115, 116] according to which both rings in naphthalene, as well as the central ring in anthracene should be more aromatic than the benzene ring, and the central ring in anthracene should be more aromatic than the outer rings. Instead, our NICS results suggest that the thiophene ring **1a** is more aromatic than the thienothiophene rings **2a** and **3a** which show levels of local aromaticity close to those of the dithienothiophene outer rings **6a** and **7a**; the central dithienothiophene rings **6b** and **7b** are less aromatic than the respective outer rings.

The changes in aromaticity between the S_0 and T_1 states of thiophene, the thienothiophenes, dithienothiophenes and sulflowers studied in this paper are, as a rule, much less pronounced than those observed in benzene, naphthalene and anthracene[105,106,108]; surprisingly, our results indicate that hexathio[6]circulene **8** which is relatively weakly aromatic in its electronic ground state becomes more aromatic in its lowest triplet state. The extents of the changes in aromaticity between the S_0 and T_1 states of the molecules we examined are reduced by the use of geometries optimised separately for the two states: It is well-known that antiaromatic molecules molecules try to 'escape' antiaromaticity through a symmetry reduction, for example, square cyclobutadiene distorts to a rectangular geometry with 'single' and 'double' carbon-carbon bonds (for a more detailed discussion and further examples, see refs. [117] and [118]). We observe well-defined Baird-style aromaticity reversals between the S_0 and T_1 states of only three of the twelve thiophene-based compounds we investigated, thieno[2,3-*b*]thiophene **2**, dithieno[3,2-*b*;2′,3′-*d*]thiophene **7** and octathio[8]circulene **10**.

Our results suggest that the geometry of thiophene changes considerably between the S_0 and T_1 states: Not only is its symmetry reduced from C_{2v} to C_s with a loss of planarity but, more importantly, the carbon-carbon 'double' and 'single' bonds in the S_0 state (see structure **1** in Figure 1) turn into 'single' and 'double' bonds, respectively, in the T_1 state. Looking for thiophene rings with geometries resembling those of a thiophene molecule in its S_0 or T_1 state can help rationalise the levels of antiaromaticity in the T_1 states of some of the compounds with fused thiophene rings studied in this paper.

Similarly to the situation observed in the T_1 state of anthracene,[106] the most antiaromatic rings in the T_1 states of dithieno[2,3-*b*:3′,2′-*d*]thiophene **6** and dithieno[3,2-*b*;2′,3′-*d*]thiophene **7** turn out to be the central rings **6b** and **7b**; the outer rings **6a** and **7b** are significantly less aromatic and very much nonaromatic, respectively. Consequently, it can be expected that in longer chains of fused aromatic rings, including thienoacenes,[119,120] T_1 antiaromaticity is likely to affect mostly the central ring (or the pair of central rings); rings sufficiently far away from the central ring(s) could even remain aromatic. This expectation is supported by the results for the T_1 states of polyacenes and phenacenes reported in ref. [121].

Acknowledgements

The authors are grateful for the support of this work by the University of York.

Conflict of Interests

The authors declare no conflict of interest.

Data Availability Statement

The data that support the findings of this study are available from the corresponding author upon reasonable request.

Keywords: sulflowers · thiophene · thienothiophenes · dithienothiophenes · aromaticity · magnetic shielding · nucleus independent chemical shifts

[1] H.-Z. Fan, X. Yang, J.-H. Chen, Y.-M. Tu, Z. Cai, J.-B. Zhu, *Angew. Chem. Int. Ed.* **2022**, *61*, e202117639.
[2] P. Chen, J. N. Metz, A. S. Mennito, S. Merchant, S. E. Smith, M. Siskin, S. P. Rucker, D. C. Dankworth, J. D. Kushnerick, N. Yao, Y. Zhang, *Carbon* **2020**, *161*, 456–465.
[3] G. Knothe, C. A. Sharp, T. W. Ryan, *Energy Fuels* **2006**, *20*, 403–408.
[4] N. Sakai, G. K. Prasad, Y. Ebina, K. Takada, T. Sasaki, *Chem. Mater.* **2006**, *18*, 3596–3598.
[5] G. Dai, J. Chang, X. Shi, W. Zhang, B. Zheng, K.-W. Huang, C. Chi, *Chem. Eur. J.* **2015**, *21*, 2019–2028.
[6] M. Hermann, R. Wu, D. C. Grenz, D. Kratzert, H. Li, B. Esser, *J. Mater. Chem. C* **2018**, *6*, 5420–5426.
[7] C. Liu, S. Xu, W. Zhu, X. Zhu, W. Hu, Z. Li, Z. Wang, *Chem. Eur. J.* **2015**, *21*, 17016–17022.
[8] C. Zhang, X. Zhu, *Acc. Chem. Res.* **2017**, *50*, 1342–1350.
[9] J. L. Eigenbrode, R. E. Summons, A. Steele, C. Freissinet, M. Millan, R. Navarro-González, B. Sutter, A. C. McAdam, H. B. Franz, D. P. Glavin, P. D. Archer, P. R. Mahaffy, P. G. Conrad, J. A. Hurowitz, J. P. Grotzinger, S. Gupta, D. W. Ming, D. Y. Sumner, C. Szopa, C. Malespin, A. Buch, P. Coll, *Science* **2018**, *360*, 1096–1101.
[10] J. Heinz, D. Schulze-Makuch, *Astrobiology* **2020**, *20*, 552–561.
[11] M. Millan, A. J. Williams, A. C. McAdam, J. L. Eigenbrode, A. Steele, C. Freissinet, D. P. Glavin, C. Szopa, A. Buch, R. E. Summons, J. M. T. Lewis, G. M. Wong, C. H. House, B. Sutter, O. McIntosh, A. B. Bryk, H. B. Franz, C. Pozarycki, J. C. Stern, R. Navarro-Gonzalez, D. P. Archer, V. Fox, K. Bennett, S. Teinturier, C. Malespin, S. S. Johnson, P. R. Mahaffy, *J. Geophys. Res. Planets* **2022**, *127*, e2021JE007107.
[12] R. Casares, Á. Martínez-Pinel, S. Rodríguez-González, I. R. Márquez, L. Lezama, M. T. González, E. Leary, V. Blanco, J. G. Fallaque, C. Díaz, F. Martín, J. M. Cuerva, A. Millán, *J. Mater. Chem. C* **2022**, *10*, 11775–11782.
[13] H. K. Saha, D. Mallick, S. Das, *Chem. Commun.* **2022**, *58*, 8492–8495.
[14] J. Usuba, M. Hayakawa, S. Yamaguchi, A. Fukazawa, *Chem. Eur. J.* **2021**, *27*, 1638–1647.
[15] J. Wirz, A. Krebs, H. Schmalstieg, H. Angliker, *Angew. Chem. Int. Ed. Engl.* **1981**, *20*, 192–193.
[16] K. E. Horner, P. B. Karadakov, *J. Org. Chem.* **2013**, *78*, 8037–8043.
[17] M. E. Cinar, T. Ozturk, *Chem. Rev.* **2015**, *115*, 3036–3140.
[18] G. A. Sotzing, M. A. Invernale, Y. Ding, *Electrochromic devices prepared from the insitu formation of conjugated polymers*, **2013**, US Patent App. 13/606,829.
[19] R. Inoue, M. Hasegawa, T. Nishinaga, K. Yoza, Y. Mazaki, *Angew. Chem. Int. Ed.* **2015**, *54*, 2734–2738.
[20] Dithieno[3,2-*b*;2′,3′-*d*]thiophene, Ambeed, https://www.ambeed.com/products/3593-75-7.html, Checked on 28/11/2023.
[21] P. B. Karadakov, *Org. Lett.* **2020**, *22*, 8676–8680.
[22] P. B. Karadakov, T. Riley, *Chem. Eur. J.* **2023**, *29*, e202203400.

[23] K. Y. Chernichenko, V. V. Sumerin, R. V. Shpanchenko, E. S. Balenkova, V. G. Nenajdenko, *Angew. Chem. Int. Ed.* **2006**, *45*, 7367–7370.
[24] N. N. Karaush-Karmazin, G. V. Baryshnikov, L. I. Valiulina, R. Valiev, H. Ågren, B. F. Minaev, *New J. Chem.* **2019**, *43*, 12178–12190.
[25] S. Hashimoto, R. Kishi, K. Tahara, *New J. Chem.* **2022**, *46*, 22703–22714.
[26] G. V. Baryshnikov, R. R. Valiev, N. N. Karaush, B. F. Minaev, *Phys. Chem. Chem. Phys.* **2014**, *16*, 15367–15374.
[27] Y. Yang, S. Helili, A. Kerim, *Mol. Phys.* **2022**, *120*, e2060146.
[28] L. H. Nguyen, *ACS Omega* **2021**, *6*, 30085–30092.
[29] B. Lousen, S. K. Pedersen, P. Bols, K. H. Hansen, M. R. Pedersen, O. Hammerich, S. Bondarchuk, B. Minaev, G. V. Baryshnikov, H. Ågren, M. Pittelkow, *Chem. Eur. J.* **2020**, *26*, 4935–4940.
[30] C. B. Nielsen, T. Brock-Nannestad, P. Hammershøj, T. K. Reenberg, M. Schau-Magnussen, D. Trpcevski, T. Hensel, R. Salcedo, G. V. Baryshnikov, B. F. Minaev, M. Pittelkow, *Chem. Eur. J.* **2013**, *19*, 3898–3904.
[31] M. Plesner, T. Hensel, B. E. Nielsen, F. S. Kamounah, T. Brock-Nannestad, C. B. Nielsen, C. G. Tortzen, O. Hammerich, M. Pittelkow, *Org. Biomol. Chem.* **2015**, *13*, 5937–5943.
[32] Y. Nagata, S. Kato, Y. Miyake, H. Shinokubo, *Org. Lett.* **2017**, *19*, 2718–2721.
[33] E. Hückel, *Z. Phys.* **1931**, *70*, 204–286.
[34] E. Hückel, *Z. Phys.* **1932**, *76*, 628–648.
[35] W. von E. Doering, F. L. Detert, *J. Am. Chem. Soc.* **1951**, *73*, 876–877.
[36] N. C. Baird, *J. Am. Chem. Soc.* **1972**, *94*, 4941–4948.
[37] W. E. Barth, R. G. Lawton, *J. Am. Chem. Soc.* **1966**, *88*, 380–381.
[38] R. G. Lawton, W. E. Barth, *J. Am. Chem. Soc.* **1971**, *93*, 1730–1745.
[39] E. Steiner, P. W. Fowler, L. W. Jenneskens, *Angew. Chem. Int. Ed.* **2001**, *40*, 362–366.
[40] W. Winter, H. Straub, *Angew. Chem. Int. Ed. Engl.* **1978**, *17*, 127–128.
[41] P. B. Karadakov, J. Gerratt, D. L. Cooper, M. Raimondi, M. Sironi, *Int. J. Quantum Chem.* **1996**, *60*, 545–552.
[42] P. V. R. Schleyer, C. Maerker, A. Dransfeld, H. Jiao, N. J. R. van Eikema Hommes, *J. Am. Chem. Soc.* **1996**, *118*, 6317–6318.
[43] M. L. McKee, M. Balci, H. Kilic, E. Yurtsever, *J. Phys. Chem. A* **1998**, *102*, 2351–2356.
[44] M. Ø. Jensen, T. Thorsteinsson, A. E. Hansen, *Int. J. Quantum Chem.* **2002**, *90*, 616–628.
[45] J. K. Pagano, J. Xie, K. A. Erickson, S. K. Cope, B. L. Scott, R. Wu, R. Waterman, D. E. Morris, P. Yang, L. Gagliardi, J. L. Kiplinger, *Nature* **2020**, *578*, 563–567.
[46] M. Gantenbein, X. Li, S. Sangtarash, J. Bai, G. Olsen, A. Alqorashi, W. Hong, C. J. Lambert, M. R. Bryce, *Nanoscale* **2019**, *11*, 20659–20666.
[47] W. Zeng, O. El Bakouri, D. W. Szczepanik, H. Bronstein, H. Ottosson, *Chem. Sci.* **2021**, *12*, 6159–6171.
[48] S. Escayola, C. Tonnelé, E. Matito, A. Poater, H. Ottosson, M. Solà, D. Casanova, *Angew. Chem. Int. Ed.* **2021**, *60*, 10255–10265.
[49] J. Aihara, *J. Am. Chem. Soc.* **1995**, *117*, 4130–4136.
[50] J. Aihara, *J. Phys. Chem.* **1995**, *99*, 12739–12742.
[51] J. Aihara, S. Oe, M. Yoshida, E. Ōsawa, *J. Comb. Chem.* **1996**, *17*, 1387–1394.
[52] J. Aihara, *J. Chem. Soc.* **1996**, 2185–2195.
[53] J. Aihara, *Phys. Chem. Chem. Phys.* **2001**, *3*, 1427–1431.
[54] J. Aihara, *J. Phys. Org. Chem.* **2008**, *21*, 79–85.
[55] J. Aihara, *J. Phys. Chem. A* **2002**, *106*, 11371–11374.
[56] J. Aihara, *Bull. Chem. Soc. Jp*$_n$. **2016**, *89*, 1425–1454.
[57] J. Aihara, *J. Am. Chem. Soc.* **1976**, *98*, 2750–2758.
[58] I. Gutman, M. Milun, N. Trinajstic, *J. Am. Chem. Soc.* **1977**, *99*, 1692–1704.
[59] J. Aihara, *Bull. Chem. Soc. Jp*$_n$. **2004**, *77*, 651–659.
[60] J. Aihara, *J. Am. Chem. Soc.* **2006**, *128*, 2873–2879.
[61] T. Ishida, H. Kanno, J. Aihara, *Polish J. Chem.* **2007**, *81*, 699–710.
[62] J. R. Dias, *J. Phys. Chem. A* **2021**, *125*, 8482–8497.
[63] H. Fliegl, S. Taubert, O. Lehtonen, D. Sundholm, *Phys. Chem. Chem. Phys.* **2011**, *13*, 20500–20518.
[64] J. Kruszewski, T. Krygowski, *Tetrahedron Lett.* **1972**, *13*, 3839–3842.
[65] T. M. Krygowski, *J. Chem. Inf. Comput. Sci.* **1993**, *33*, 70–78.
[66] C. Bird, *Tetrahedron* **1985**, *41*, 1409–1414.
[67] J. Pedersen, K. V. Mikkelsen, *RSC Adv.* **2022**, *12*, 2830–2842.
[68] M. Cyrański, T. M. Krygowski, *Tetrahedron* **1998**, *54*, 14919–14924.
[69] E. M. Arpa, B. Durbeej, *Phys. Chem. Chem. Phys.* **2023**, *25*, 16763–16771.
[70] M. Bühl, C. van Wüllen, *Chem. Phys. Lett.* **1995**, *247*, 63–68.
[71] E. Matito, J. Poater, M. Duran, M. Solà, *J. Mol. Struct.* **2005**, *727*, 165–171.
[72] J. C. Dobrowolski, P. F. Lipiński, *RSC Adv.* **2016**, *6*, 23900–23904.
[73] P. Lazzeretti, *Phys. Chem. Chem. Phys.* **2004**, *6*, 217–223.
[74] C. Foroutan-Nejad, S. Shahbazian, F. Feixas, P. Rashidi-Ranjbar, M. Solà, *J. Comput. Chem.* **2011**, *32*, 2422–2431.
[75] C. Foroutan-Nejad, *Theor. Chem. Acc.* **2015**, *134*, 1–9.
[76] S. Fias, P. W. Fowler, J. L. Delgado, U. Hahn, P. Bultinck, *Chem. Eur. J.* **2008**, *14*, 3093–3099.
[77] S. Van Damme, G. Acke, R. W. Havenith, P. Bultinck, *Phys. Chem. Chem. Phys.* **2016**, *18*, 11746–11755.
[78] K. Wolinski, *J. Chem. Phys.* **1997**, *106*, 6061–6067.
[79] S. Klod, E. Kleinpeter, *J. Chem. Soc.* **2001**, 1893–1898.
[80] P. B. Karadakov, B. VanVeller, *Chem. Commun.* **2021**, *57*, 9504–9513.
[81] C. Lee, W. Yang, R. G. Parr, *Phys. Rev. B* **1988**, *37*, 785–789.
[82] A. D. Becke, *J. Chem. Phys.* **1993**, *98*, 5648–5652.
[83] P. J. Stephens, F. J. Devlin, C. F. Chabalowski, M. J. Frisch, *J. Phys. Chem.* **1994**, *98*, 11623–11627.
[84] S. H. Vosko, L. Wilk, M. Nusair, *Can. J. Phys.* **1980**, *58*, 1200–1211.
[85] S. Grimme, S. Ehrlich, L. Goerigk, *J. Comb. Chem.* **2011**, *32*, 1456–1465.
[86] F. Weigend, R. Ahlrichs, *Phys. Chem. Chem. Phys.* **2005**, *7*, 3297–3305.
[87] O. Ivasenko, J. M. MacLeod, K. Y. Chernichenko, E. S. Balenkova, R. V. Shpanchenko, V. G. Nenajdenko, F. Rosei, D. F. Perepichka, *Chem. Commun.* **2009**, 1192–1194.
[88] F. London, *J. Phys. Radium* **1937**, *8*, 397–409.
[89] R. McWeeny, *Phys. Rev.* **1962**, *126*, 1028–1034.
[90] R. Ditchfield, *Mol. Phys.* **1974**, *27*, 789–807.
[91] K. Wolinski, J. F. Hinton, P. Pulay, *J. Am. Chem. Soc.* **1990**, *112*, 8251–8260.
[92] J. R. Cheeseman, G. W. Trucks, T. A. Keith, M. J. Frisch, *J. Chem. Phys.* **1996**, *104*, 5497–5509.
[93] A. D. McLean, G. S. Chandler, *J. Chem. Phys.* **1980**, *72*, 5639–5648.
[94] K. Raghavachari, J. S. Binkley, R. Seeger, J. A. Pople, *J. Chem. Phys.* **1980**, *72*, 650–654.
[95] A. J. H. Wachters, *J. Chem. Phys.* **1970**, *52*, 1033–1036.
[96] P. J. Hay, *J. Chem. Phys.* **1977**, *66*, 4377–4384.
[97] K. Raghavachari, G. W. Trucks, *J. Chem. Phys.* **1989**, *91*, 1062–1065.
[98] V. Gogonea, P. v. R. Schleyer, P. R. Schreiner, *Angew. Chem. Int. Ed.* **1998**, *37*, 1945–1948.
[99] P. Fowler, E. Steiner, L. Jenneskens, *Chem. Phys. Lett.* **2003**, *371*, 719–723.
[100] Z. Rinkevicius, J. Vaara, L. Telyatnyk, O. Vahtras, *J. Chem. Phys.* **2003**, *118*, 2550–2561.
[101] J. Vaara, *Phys. Chem. Chem. Phys.* **2007**, *9*, 5399–5418.
[102] M. J. Frisch, G. W. Trucks, H. B. Schlegel, G. E. Scuseria, M. A. Robb, J. R. Cheeseman, G. Scalmani, V. Barone, G. A. Petersson, H. Nakatsuji, X. Li, M. Caricato, A. V. Marenich, J. Bloino, B. G. Janesko, R. Gomperts, B. Mennucci, H. P. Hratchian, J. V. Ortiz, A. F. Izmaylov, J. L. Sonnenberg, D. Williams-Young, F. Ding, F. Lipparini, F. Egidi, J. Goings, B. Peng, A. Petrone, T. Henderson, D. Ranasinghe, V. G. Zakrzewski, J. Gao, N. Rega, G. Zheng, W. Liang, M. Hada, M. Ehara, K. Toyota, R. Fukuda, J. Hasegawa, M. Ishida, T. Nakajima, Y. Honda, O. Kitao, H. Nakai, T. Vreven, K. Throssell, J. A. Montgomery, Jr., J. E. Peralta, F. Ogliaro, M. J. Bearpark, J. J. Heyd, E. N. Brothers, K. N. Kudin, V. N. Staroverov, T. A. Keith, R. Kobayashi, J. Normand, K. Raghavachari, A. P. Rendell, J. C. Burant, S. S. Iyengar, J. Tomasi, M. Cossi, J. M. Millam, M. Klene, C. Adamo, R. Cammi, J. W. Ochterski, R. L. Martin, K. Morokuma, O. Farkas, J. B. Foresman, D. J. Fox, *Gaussian 16 Revision C.01*, **2016**, Gaussian Inc. Wallingford CT.
[103] T. Lu, F. Chen, *J. Comb. Chem.* **2012**, *33*, 580–592.
[104] Z. Chen, C. S. Wannere, C. Corminboeuf, R. Puchta, P. v. R. Schleyer, *Chem. Rev.* **2005**, *105*, 3842–3888.
[105] P. B. Karadakov, *J. Phys. Chem. A* **2008**, *112*, 7303–7309.
[106] P. B. Karadakov, M. A. Al-Yassiri, *J. Phys. Chem. A* **2023**, *127*, 3148–3162.
[107] P. B. Karadakov, K. E. Horner, *J. Phys. Chem. A* **2013**, *117*, 518–523.
[108] P. B. Karadakov, P. Hearnshaw, K. E. Horner, *J. Org. Chem.* **2016**, *81*, 11346–11352.
[109] P. B. Karadakov, K. E. Horner, *J. Chem. Theory Comput.* **2016**, *12*, 558–563.
[110] P. B. Karadakov, J. Kirsopp, *Chem. Eur. J.* **2017**, *23*, 12949–12954.
[111] S. Pelloni, A. Ligabue, P. Lazzeretti, *Org. Lett.* **2004**, *6*, 4451–4454.
[112] P. B. Karadakov, *Chemistry* **2021**, *3*, 861–872.
[113] P. v. R. Schleyer, M. Manoharan, H. Jiao, F. Stahl, *Org. Lett.* **2001**, *3*, 3643–3646.
[114] G. Portella, J. Poater, J. M. Bofill, P. Alemany, M. Solà, *J. Org. Chem.* **2005**, *70*, 2509–2521.
[115] P. Bultinck, *Faraday Discuss.* **2007**, *135*, 347–365.
[116] P. W. Fowler, W. Myrvold, *J. Phy. Chem. A* **2011**, *115*, 13191–13200.

[117] C.-H. Wu, L. J. Karas, H. Ottosson, J. I.-C. Wu, *Proc. Natl. Acad. Sci. USA* **2019**, *116*, 20303–20308.
[118] L. J. Karas, J. I.-C. Wu, in *Aromaticity*, I. Fernandez (Ed.), Elsevier, **2021**, pp. 319–338.
[119] K. Xiao, Y. Liu, T. Qi, W. Zhang, F. Wang, J. Gao, W. Qiu, Y. Ma, G. Cui, S. Chen, X. Zhan, G. Yu, J. Qin, W. Hu, D. Zhu, *J. Am. Chem. Soc.* **2005**, *127*, 13281–13286.
[120] K. Takimiya, S. Shinamura, I. Osaka, E. Miyazaki, *Adv. Mater.* **2011**, *23*, 4347–4370.
[121] R. Pino-Rios, R. Báez-Grez, M. Solà, *Phys. Chem. Chem. Phys.* **2021**, *23*, 13574–13582.

Manuscript received: November 9, 2023
Accepted manuscript online: December 1, 2023
Version of record online: ■■, ■■

RESEARCH ARTICLE

Off-nucleus isotropic shielding isosurfaces computed with DFT show that while the sulflower with eight thiophene rings follows Baird's rule by switching from aromatic in its electronic ground state to antiaromatic in its lowest triplet state, the sulfower with six thiophene rings disobeys the rule by becoming even more aromatic in its lowest triplet state.

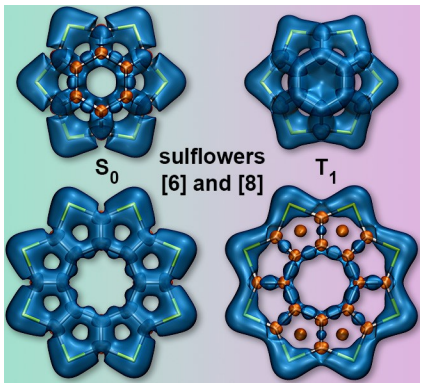

*E. Cummings, Prof. Dr. P. B. Karadakov**